Modeling a Grid Connected Photovoltaic System with Perturb and Observe based Maximum Power Point Tracking

Anant Naik & Udaykumar Yaragatti

Published online: 24 Sep 2013.

Submit your article to this journal ↗

Article views: 187

View related articles ↗

Citing articles: 1 View citing articles ↗

Modeling a Grid Connected Photovoltaic System with Perturb and Observe based Maximum Power Point Tracking

Anant Naik, Udaykumar Yaragatti

ABSTRACT

This article deals with the integration study of distributed generation (DG) in the form of a photovoltaic (PV) plant in a three-phase system. Here the active power generated by the photovoltaic (PV) plant is injected into the grid system through a current controlled dual inverter topology. The main contribution in this article is the dual inverter topology. In this topology, a three level inverter output is obtained which reduces the PV injected current harmonic distortion into the grid. The control algorithm used in this article is simple and easy to implement. The PV system is operated through a maximum power point tracking (MPPT) stage. Perturb & Observe (P&O) is the modeling approach of MPPT system operation. The system is simulated and analyzed for a different set of loads with renewable source at different atmospheric conditions using MATLAB/ Simulink tool. The grid current becomes sinusoidal with three levels inverter and compared to existing three levels methods the dual inverter method is simple and easy to implement.

Keywords: current controlled voltage source inverter, distributed generation, dual inverter, maximum power point tracking, perturb and observe, photovoltaic, three level inverter,

INTRODUCTION

The reduction in carbon emissions is one of the primary goals of smart energy. Grid-connected renewable power is the main path through which such goals can be achieved. The distributed generation (DG) concept is

becoming more and more popular as it can provide more reliability, reduced emissions and provide additional power quality benefits [1]. Photovoltaic (PV) energy is abundant in nature and is available everywhere. Hence PV energy is one of the attractive sources of energy. Unfortunately, PV generation system suffers from disadvantages such as poor conversion efficiency, weather dependant and nonlinear I-V characteristics. Therefore it is very much essential to extract maximum available power from the PV array. Several maximum power point tracking (MPPT) algorithms are reported in the literature [2]-[5]. When operated in grid connected mode the inverter is current controlled as the voltage at the point of common coupling (PCC) is imposed by the grid. Here the PV system injects only the active power to the grid through inverter and the reference current is computed from active power that PV system generates at a given time [6].

   In the grid connected renewable sources the major issue concern is the quality of current injected at PCC. This injected current also affects the grid current and hence it is required to inject current with minimum distortion. The quality of current can be improved if we can use multilevel voltage source inverters (VSI) at the conversion stage. Cascaded converter, together with the diode clamped and capacitor clamped converters, makes the three most common types of present multilevel topologies [7], [8]. Cascaded converters still receives large attention among these topologies, due to the simplicity of the power stage not requiring additional components such as diodes and capacitors. Cascaded topology provides the same number of output voltage levels using two yet simpler multilevel inverters instead of one complex inverter with large number of leg levels. In dual inverter topology, the two inverters are connected "in opposition" at two ends of the load in order to obtain output voltage as a difference of inverter's leg potentials. The benefit of dual inverter arises from the fact that use of components with lower voltage ratings enables bigger efficiency. The dual inverter configuration consists of the simple connection of two standard 2-level inverters to a three-phase open-winding load, and performs as a 3-level inverter. Although it is not scalable to get more voltage levels, it represents a viable solution to supply transformers and ac motors, especially when the dc source can be easily split in two insulated parts, as for batteries and PV panels [9].

   In this article, a three-phase, grid- interactive PV system with dual inverter three-level VSI is proposed. The idea is to integrate PV system such that the dual inverter feeds the open end primary of a three phase transformer which also acts as filter inductor. With this topology, hence

more PV power is injected with two sources connected at the inputs of the two inverters. The three-phase, grid interactive PV system along with its MPPT algorithm and three-level dual inverter is modeled and simulated in MATLAB/Simulink environment. Section II covers brief description of the system. PV modeling and its characteristics are covered in section III. The control method and SV-PWM for dual inverter is explained in sections IV and V respectively. Section VI gives simulation results and conclusion is given in section VII.

SYSTEM DESCRIPTION

The system being studied is shown in Figure 1. It consists of a dual inverter feeding open end primary of a three phase transformer. The star connected secondary of this transformer is connected to PCC. Two PV sources are connected at the two inputs of the VSIs. They feed current into the grid and the local load through transformer inductance L which acts as filter inductance. The output DC voltage of PV cell is maintained constant by capacitor Cdc at the input of the inverter.

PV MODELING AND ITS CHARACTERISTICS

The electrical output from the PV cell is described by the I-V characteristics whose parameters can be linked to the material properties of the semiconductor. These I-V characteristics of solar cell can be obtained by drawing an equivalent circuit of the device as shown in the Figure 2 [10], [11].

The generation of current I_{ph} by light is represented by a current generator in parallel with a diode which represents the p-n junction. The output current I_c is then equal to the difference between the light generated current I_{ph} and the diode current I_d. In practical applications, solar cells do not operate under standard conditions. The two most important effects that must be allowed for are due to the variable temperature and irradiance. Most frequently, the PV cells in a module are interconnected in series. The number of cells in a module is governed by the voltage of the module. The three most important electrical characteristics of a module are the short circuit current, open circuit voltage and the maximum power point as function of temperature and irradiance. To simulate PV array, the
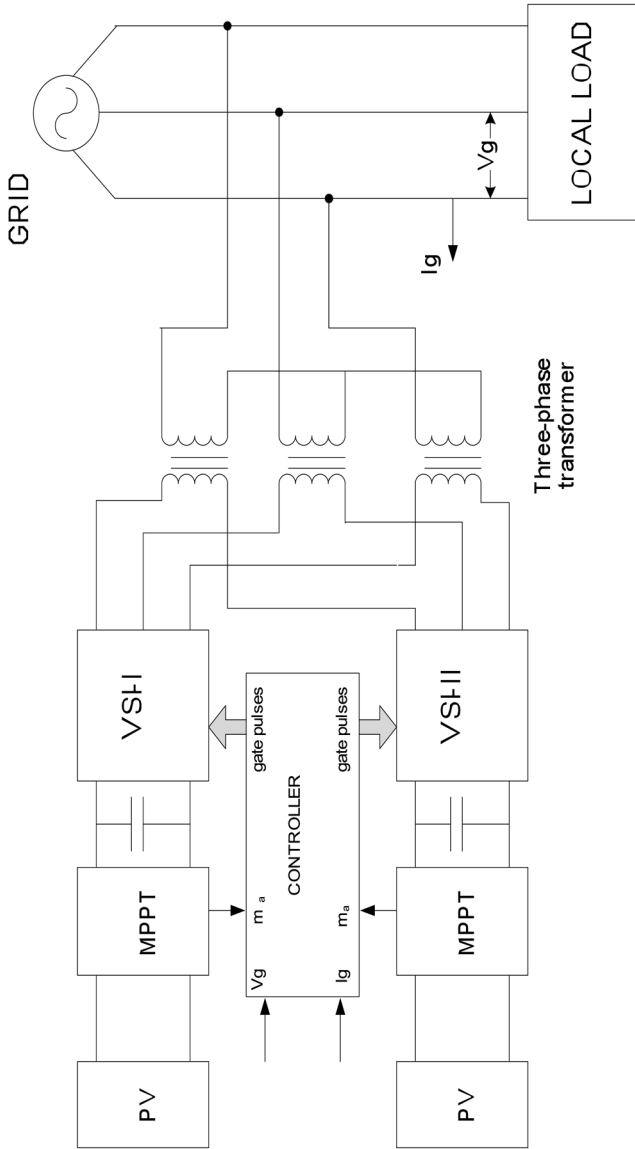
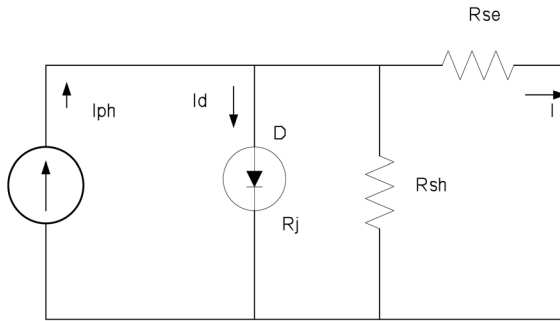**Figure 1. Grid connected PV system**

Figure 2. Equivalent circuit of PV module.

mathematical model neglecting shunt resistance R_{sh} is used according to the following set of equations:

The output voltage of PV cell is a function of photo current and it depends upon solar insolation level.

$$V_C = \frac{AkT_c}{e} \ln\left(\frac{I_{ph} + I_d - I_c}{I_d}\right) - R_{se} + I_c \tag{1}$$

where, I_c and V_c are cell output current and voltage, respectively; I_d is the reverse saturation current of the diode; T_c is the cell temperature at standard test conditions (STC) in °C; k is Boltzmann's constant in J/°C; e is electronic charge; I_{ph} is the light-generated current; A=1.92 is ideality factor; R_{se} is the series resistance. The array voltage is obtained by multiplying equation (1) by the number of the cells connected in series, N_s. The array current is obtained by multiplying the cell current by the number of the cells connected in parallel, N_p. This value of current is valid for a certain cell operating temperature T_c and its corresponding solar insolation level S_c. A method to include the effects of the changes in temperature and solar insolation levels is given in [12]. According to this, a model is obtained for known temperature (T_c) and solar insolation (S_c). The solar cell operating temperature varies as a function of solar insolation level and ambient temperature. The cell output voltage and cell photocurrent are affected by ambient temperature. These effects are represented by temperature coefficients C_{TV} and C_{TI} for cell output voltage and cell photocurrent respectively.

$$C_{TV} = 1 + \beta_T(T_a - T_x) \tag{2}$$

$$C_{TI} = 1 + \frac{Y_T}{S_c} \ (T_x - T_a) \tag{3}$$

where T_a and S_a are ambient temperature and cell solar insolation level at STC, respectively. T_x is any other temperature. β_T and Y_T are constants specified by the manufacturers. Similarly, the change in solar insolation level causes a change in the cell photocurrent and operating temperature. Therefore, the change in the cell output voltage and the cell photocurrent are corrected by the two factors,

$$C_{SV} = 1 + \beta_T \alpha_s (S_x - S_a) \tag{4}$$

$$C_{SI} = 1 + \frac{1}{S_c} \ (S_x - S_a) \tag{5}$$

where, S_x is the new level of solar insolation. α_s represents the slope of the change in the solar insolation level. Using correction factors given in Equations (2)-(5), the new values of cell output voltage V_{cx} and photocurrent I_{phx} are given for any temperature T_x and solar insolation S_x as

$$V_{cx} = C_{TV} C_{SV} V_c \tag{6}$$

$$I_{phx} = C_{TI} C_{SI} I_{ph} \tag{7}$$

where, V_c and I_{ph} are the cell output voltage and photocurrent at S_{TC}, respectively.

The rating of a P_V module is estimated by the maximum power at S_{TC} which corresponds to an insolation level of 1000 W/m² and a cell temperature of 25°C. The PV cell manufacturers provides its characteristics by specifying the parameters given in Table 1.

Table 1. Specifications for solar array at STC

Parameter	Value
Isc	3.74 A
Voc	21 V
Pm	61.85 W
Im	3.5 A
Vm	17.1 V

Module: Solarex MSX60, 60 W PV module at STC irradiance: 1000W / sq.m, ambient temp: 25°C.

The maximum power point operation of a PV array is achieved by maximizing its output power to load. To obtain a maximized output power, controllers are used to minimize the error between the operating power and the reference maximum power. The maximum power must be determined for the changing temperature and solar irradiation level before it is compared with the operating power. The MPPT method used here is Perturb & Observe. (P&O)

CONTROL METHOD

The proposed inverter is used in a grid connected PV system. Therefore a PI controller is used to keep the output current sinusoidal and to have high dynamic performance under rapidly changing atmospheric condition. The amount of electric power generation by solar module is always changing with weather condition. To extract the maximum power at any given atmospheric conditions, MPPT is used. Therefore MPPT algorithm will ensure that maximum power is delivered from solar module. Here perturb & observation (P&O) algorithm is used to extract maximum power from PV module.

P&O algorithm as shown in Figure 3 is very popular because of its simplicity and ease of implementation [13]. Basically, the module current is perturbed by a small increment, and the resulting change in the power is observed. If the change in power is positive, the current is adjusted by the same increment, and the power is again observed. This continues until the change in power is negative, at which point the direction of the change in current is reversed.

The MPPT controller takes V_{pv} and I_{pv} as inputs to detect power slope and generates V_{ref} to track the maximum power point. This V_{ref} is then used to generate firing pulses for the DC-DC converter in closed loop system as shown in Figure 4.

The feedback controller used in this application utilized the PI algorithm [14]. As shown in Figure 5 the current injected into the grid I_g is sensed and fed back to a comparator which compares it with the reference current I_{ref}. I_{ref} is obtained by measuring the grid voltage and multiplying it with variable m_a. Therefore,
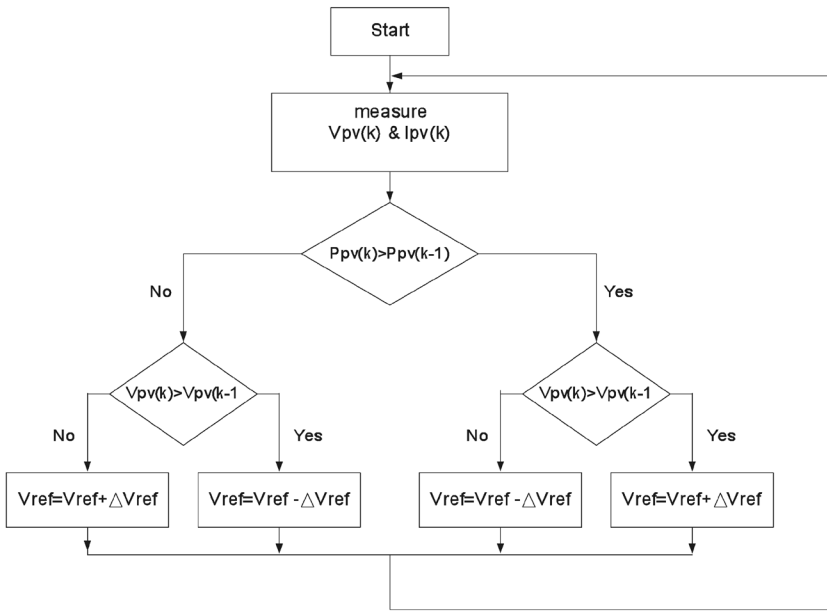
$$I_{ref} = m_a V_g \qquad\qquad\qquad (8)$$

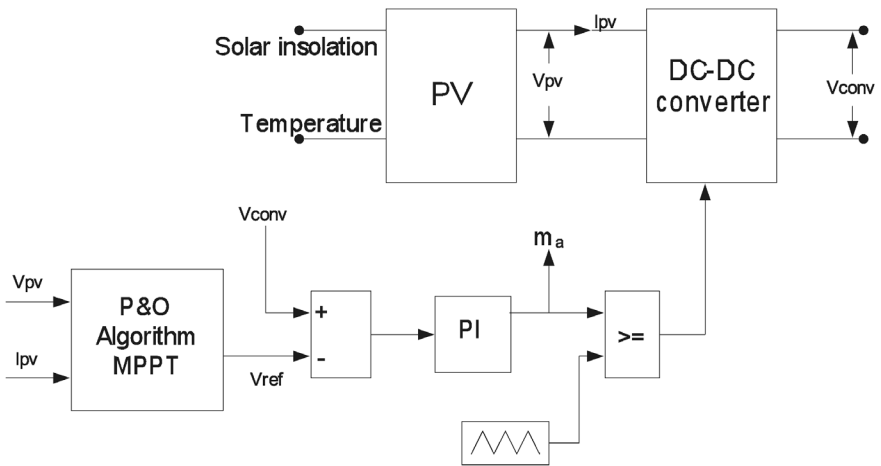**Figure 3: Perturb and Observe algorithm**

Figure 4: control of DC-DC converter to obtain maximum power from PV system

Here m_a is a modulation index obtained from MPPT to generate I_{ref}. As variable m_a is dependent on the solar irradiation, therefore,
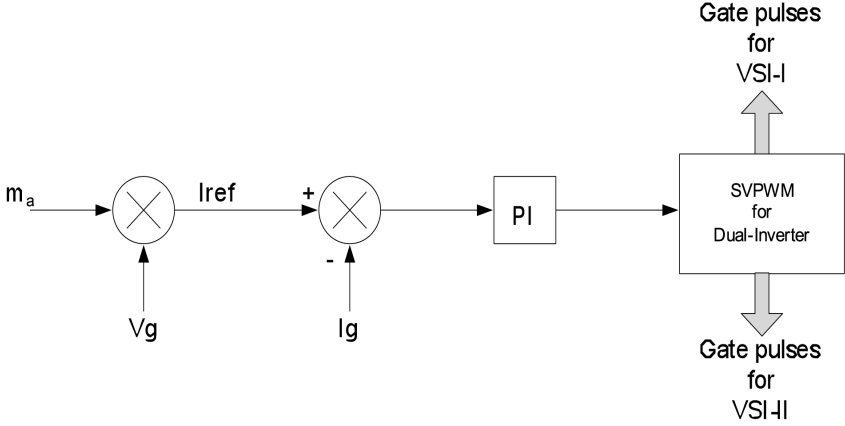
$$m_a \ \alpha \ \text{solar irradiation}$$

Figure 5. Controller used to generate firing pulses for two inverters

The PI algorithm, can be expressed in the continuous time domain as,

$$U(t) = K_p e(t) + K_i \int_{r-o}^{1} e(\tau)dt \tag{9}$$

where

error e(t)   = setpoint-plant output
    Kp   = Proportional gain
    Ki   = Integral gain

SV-PWM FOR DUAL INVERTER

A new multilevel topology is being used to drive induction motor namely open-end winding induction motor drive [15]. Based on similar lines a dual fed three phase transformer is used here in place of an induction motor. Out of six free terminals of primary winding of this transformer, three ends are fed from VSI-I and other three free ends are fed from VSI-II as shown in Figure 6. The state phasor locations from individual inverters are shown in Figure 7.
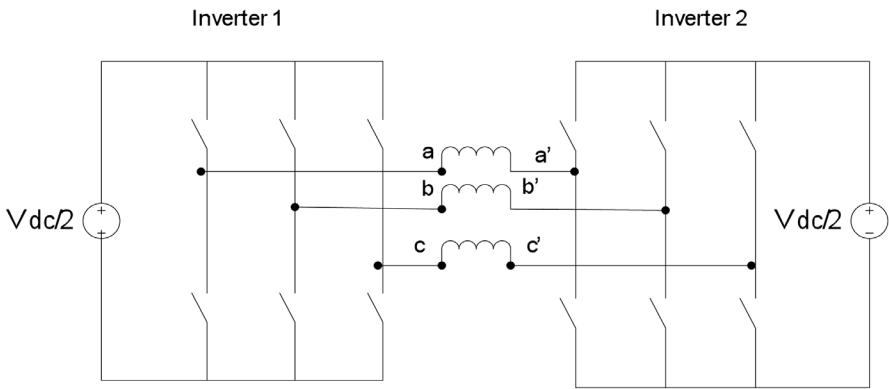
Inverter 1   Inverter 2

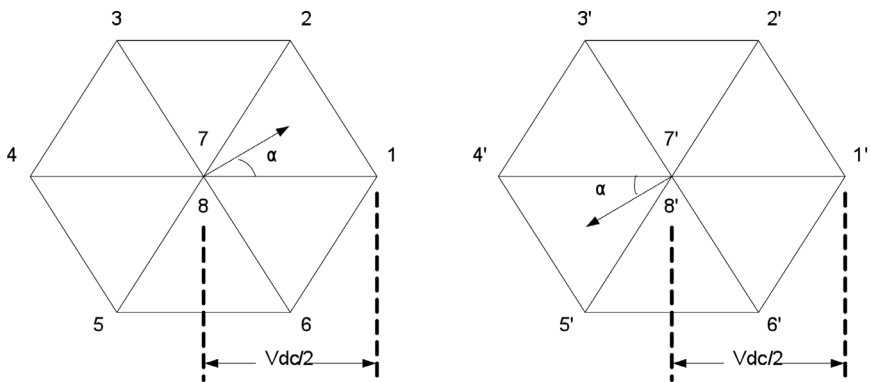**Figure 6. Open end fed primary winding of transformer**

Figure 7. Voltage vector locations for inverter –I and II

The control strategy of these two inverters is selected such that three level output voltage is generated across each phase of the transformer primary. The star connected secondary of this transformer is connected to the PCC so that the transformer acts as filter inductance. The DC link voltage of each inverter is $V_{dc}/2$, which is the output from PV panels. The space phasor combinations ($2^3 X 2^3 = 26 = 64$) as each inverter is assumed with 8 states independently of each other) from the 2 inverters is shown in Figure 8. In the Figure 8, the |OA| represents the DC link voltage of individual inverters and is equal to the $V_{dc}/2$ while |OG| represents the DC link voltage of an equivalent single

inverter drive and is equal to V_{dc}. It can be observed that the switching locations are similar to the conventional NPC inverter scheme. It can be also observed that the core hexagon ABCDEF with centered O, can be plot by single inverter to obtain the other hexagons with centers A, B, C, D, E, F respectively. The hexagons namely OBHGSF, OCJIHA, ODLKJB, OENMLC, OFQPND and OASRQE are called as sub-hexagons. The centers A, B, C, D, E, F are called as sub-hexagons centers (SHCs). The resultant space vector combination locations shown in Figure 8 are obtained by superposing the space vector locations resulting from the inverter-2 at each space vector location caused by the inverter-1. All the seven locations of a given sub hexagonal center (i.e., six vertices and the corresponding sub hexagonal center) show redundancy of space vector combinations. For the subhexagon OFSGHB, the space vector combinations for these seven locations may alternatively be obtained by clamping inverter-2 to state -4 (- + +) while the other inverter switches in all eight states.
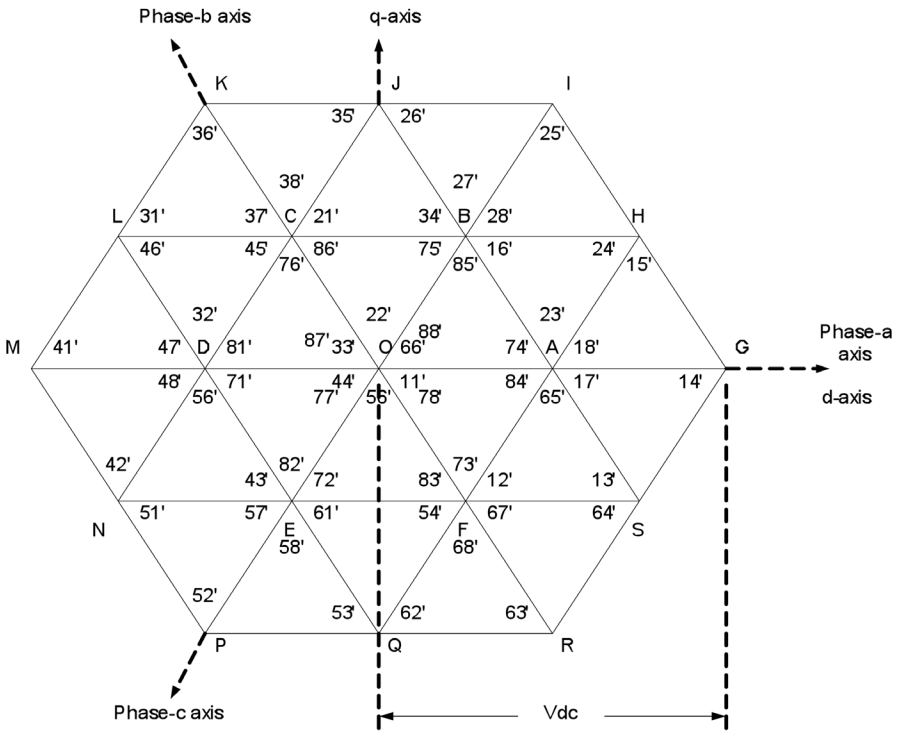

Figure 8. Voltage vector positions in three-level inverter.

Nearest Sub-hexagon Switching Scheme [16]

This scheme is based on the observation that the space vector combinations at the vertices and the center of a given sub hexagon are obtained by clamping one inverter with an active state, while the other inverter switches in all eight states. The center of the nearest sub hexagon is obtained from the instantaneous reference voltage quantities. In the Figure 9, vector OT represents the reference vector with its tip located in sector 7 (in the triangle AHG). It is resolved into two components OA and AT. The vector OA may be output of inverter-1 which is clamped to state 1 (+ - -) through the sampling interval and the vector AT may be the output of other inverter-2, which is switched in all eight states. In other words, the inverter-2 is switched with center A (the nearest sub hexagon center of OFSGHB). Otherwise the first vector OA is the output of the inverter-2 which is clamped to the state 1(+ - -) and the
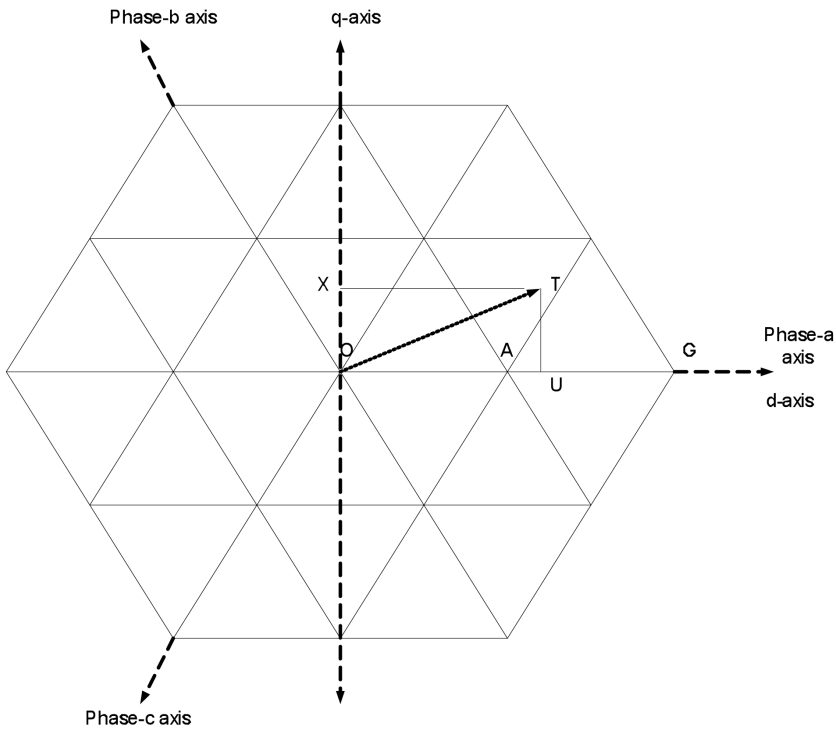

Figure 9. Switching vector components along d and q axis

vector AT is the generated by switching the inverter-1. At each step of the interval the nearest sub hexagon center is identified by resolving the OT vector in to two components and first component is the output of the one inverter by clamped to an active state and other inverter is switched in all eight centers. In this scheme for the odd numbered centers inverter-1 is clamped i.e., for A, C, E sub hexagon centers and the inverter -2 is switched, and for the other centers i.e., B, D, F center sub hexagons inverter-2 is clamped and inverter-1 is switched. The roles of the individual inverters at each center are summarized in Table 2.

The instantaneous phase reference voltage denoted by Vas, Vbs, Vcs corresponding to the reference voltage space vector OT are obtained by projecting the tip of OT onto the respective phase axes and multiplying them by a factor (2/3). The symbols Vds and Vqs denote the components of OT on the d and q axes, respectively. The reference voltages corresponding to the actual switching vector AT, denoted by Va, Vb and Vc, are obtained by the following procedure:

1. By using classical 3 phase to 2 phase transformation method we can obtain the equivalent two-phase system references Vds and Vqs of the reference vector OT from the instantaneous phase reference voltages Vas, Vbs and Vcs.
2. The Sub Hexagonal Center situated nearest to the tip of the reference vector OT is then determined.
3. The coordinates of the nearest Sub Hexagonal Center (NSHC) in the Vd – Vq plane (the point 'A' in this example, Figure 9, denoted by Vdnshc and Vqnshc are identified for all the six Sub Hexagonal Center s. For example, the coordinates of the point

Table 2. roles of each inverter in NSH centers

NSHC	A	B	C	D	E	F
Inverter - 1	Clamped to state-1(+--)	Switching mode	Clamped to state-3(-+-)	Switching mode	Clamped to state-5(--+)	Switching mode
Inverter - 2	Switching mode	Clamped to state-2(++-)	Switching mode	Clamped to state-4(-++)	Switching mode	Clamped to state-6(+-+)

'A' in the Vd –Vq plane are given by (Vdc/2, 0), similarly the coordinates of the point 'D' in the Vd –Vq plane are given by (-Vdc/2, 0).

4. Since the vector OA is output by the clamping inverter, the coordinates of the switching vector (AT in the present case) denoted by Vdsw and Vqsw are given by

$$Vdsw = Vds - Vdnshc \qquad\qquad (11)$$

$$and \;\; Vqsw = Vqs - Vqnshc \qquad\qquad (12)$$

5. By using the classical two-phase to three-phase transformation, the modified reference phase voltages Vasw, Vbsw and Vcsw for the switching inverter are then obtained by transforming Vdsw, Vqsw into the corresponding three-phase variables.

6. If inverter-2 is employed as the clamping inverter, the modified references are used directly to generate the switching vector AT with inverter-1. On the other hand, if inverter-1 is used as the clamping inverter, it is obvious that the modified references must be negated to generate the switching vector AT with inverter-2.

7. It is important to note that the most important part of this algorithm is to find the nearest sub hexagonal center to the tip of the reference vector OT. By finding the maximum value amongst the six phasors (V_{as},-V_{as},V_{bs},-V_{bs},V_{cs},-V_{cs}) quantities, one can determine the nearest sub hexagonal center.

The overall SVPWM algorithm of a dual inverter is shown in Figure 10. The reference signal generated by the control method used is initially transformed into its 2-phase equivalent. The magnitude and angle of this reference signal is obtained using rectangular to polar transformation block available in the simulation tool of MATLAB/ Simulink. The angle of the reference signal provides the information about the sector in which the reference signal lies at any sampling instant. Also the angle information is used to find the NSHC using the step 7 of the above mentioned algorithm. The coordinates of each of the NSHCs are known in advance and hence this data is used to generate switching signals for a clamping inverter. Depending upon the location
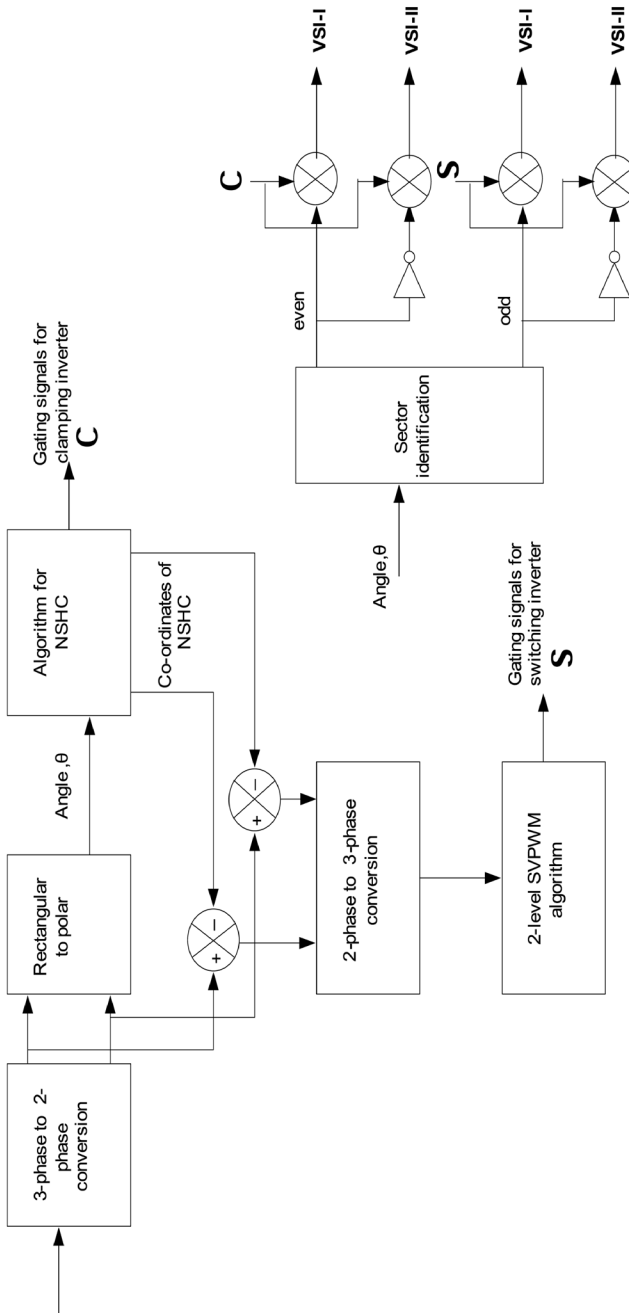
Figure 10. dual inverter SVPWM functional diagram

of reference signal vector, the d and q axis coordinates of the sub hexagon centre are subtracted from the coordinates of the reference vector. These data are then converted into three phase equivalent and samples for switching inverter are generated using normal 2-level SVPWM algorithm. In this way the gating signals for the two inverters (clamping and switching) are generated at every sampling instants. The function of each inverter i.e. inverter-I and inverter-II is again decided by the location of reference vector or sector.

RESULTS AND DISCUSSIONS

The various parameters used for simulation are given in Table 3.
Figures 11, 12 and 13)show the operation of this system in different modes.

Mode I: Here the system operates without PV power injection. From Figure 11 it is clear that the source current is equal to load current. This can be seen from t = 0 to t = 0.1 sec. Figure 12 shows that active power demand of the load is supplied by the grid. Figure (13) shows the dual inverter phase voltage during this interval.

Mode II: From t = 0.1 sec to 0.2 sec, VSI is connected to the system with 320W of PV power generation. The corresponding grid, PV and load currents are shown in Figure 11. Now the grid current is reduced. The active power is shared by grid and PV as shown in Figure 12. There is slight increase in the grid active power demand as VSI draws fraction of active power to overcome inverter losses.

Table 3. Simulation Parameters

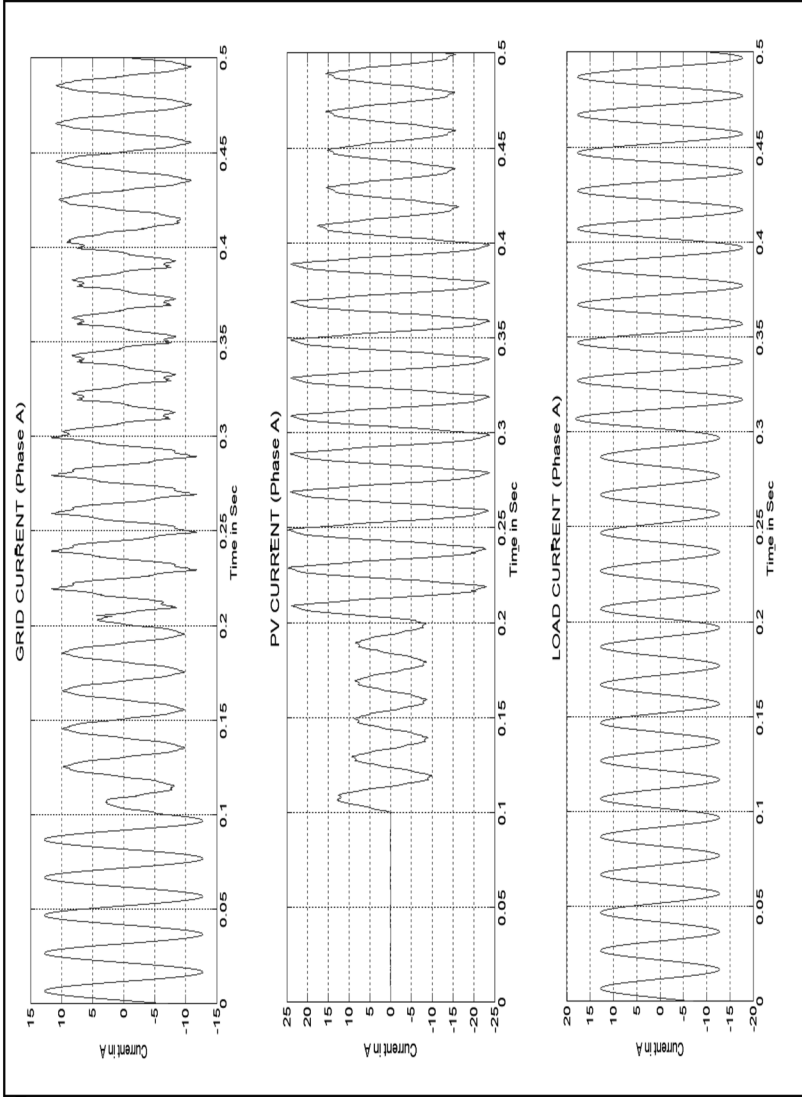| Location	Parameter	Value
PV	Total no of modules	NsxNp=15x4=60
	Maximum power generated by	200x60 ≈ 12000
	PV array	W
Interconnecting Transformer	Open primary, star connected secondary	10kVA, 500V/500V
Grid	Grid voltage at 50 Hz	230 V
Load	(i)Three phase R-L load	5 kVA
	(ii)Three phase R-L load	5kVA+1.7kVA

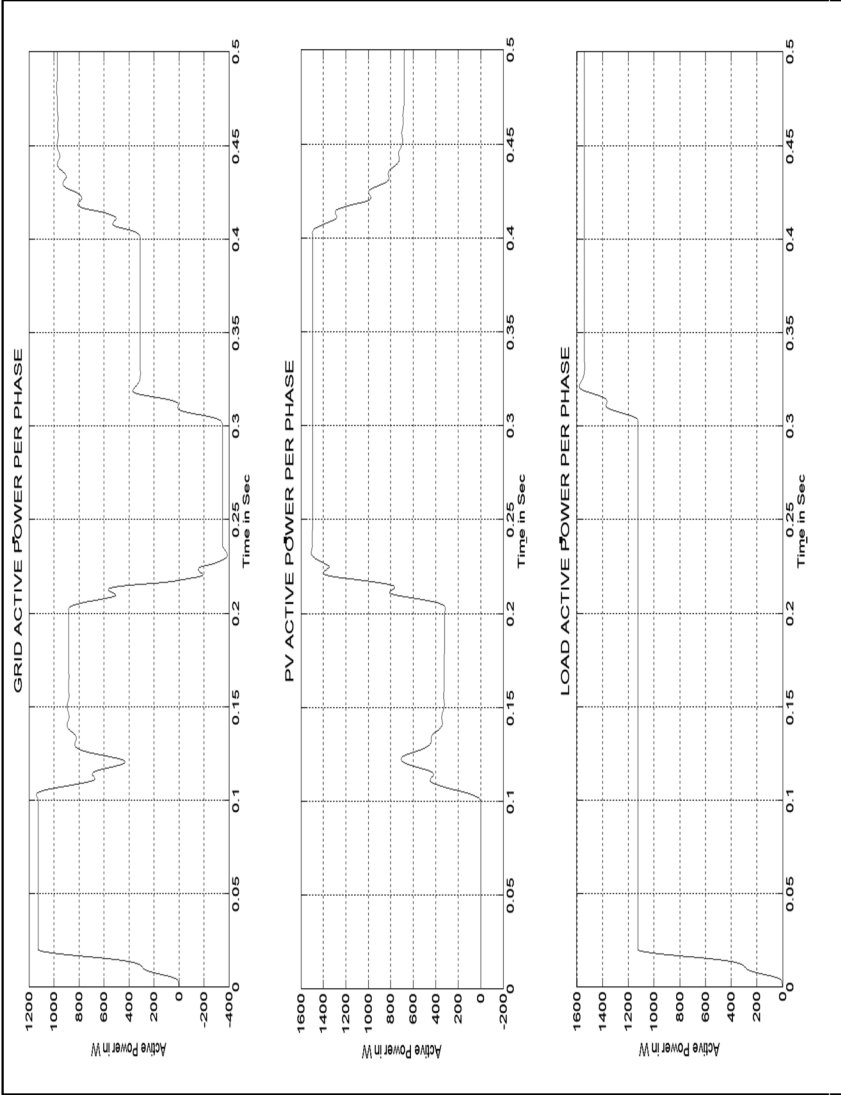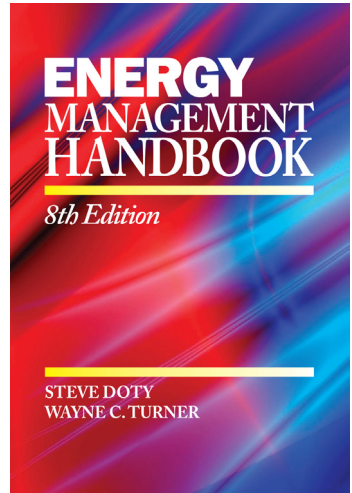**Figure 11. Currents at different points**

Figure 12. Active power distribution

ENERGY MANAGEMENT HANDBOOK, 8th Edition

Steve Doty and Wayne C. Turner

This comprehensive handbook has become recognized as the definitive stand-alone energy manager's desk reference, used by thousands of professionals throughout the industry. Newly revised and edited, this eighth edition includes significant updates to energy management controls systems, commissioning, measurement and verification, and high performance green buildings. Also updated are chapters on motors and drives, HVAC systems, lighting, alternative energy systems, building envelope, performance contracting and natural gas purchasing. You'll find coverage of every component of effective energy management, including energy auditing, economic analysis, boilers and steam systems, heat recovery, cogeneration, insulation, thermal storage, indoor air quality, utility rates, energy systems maintenance, and more. Detailed illustrations, charts and other helpful working aids are provided throughout.

ENERGY MANAGEMENT HANDBOOK
8th Edition
STEVE DOTY
WAYNE C. TURNER

ISBN: 0-88173-707-0

8½ x 11, 839 pp., Illus.
Hardcover, Order Code: 0674

————CONTENTS————

BOOK ORDER FORM — — — — — — — — — — — — ✂

① Complete quantity and amount due for each book you wish to order:

Quantity	Book Title	Order Code	Price	Amount Due
	Energy Management Hankbook, 8th Edition	**0674**	**$260.00**	

② Indicate shipping address: CODE: Journal 2013

Applicable Discount

Georgia Residents add 6% Sales Tax

Shipping $10 first book, $4 each additional book

TOTAL

NAME (Please print)   BUSINESS PHONE

SIGNATURE (Required to process order)   EMAIL ADDRESS

COMPANY

STREET ADDRESS ONLY (No P.O. Box)

CITY, STATE, ZIP

MEMBER DISCOUNTS—A 15% discount is allowed to AEE members (discounts cannot be combined).
☐ AEE Member (Member No._____)

③ Select method of payment:
☐ CHECK ENCLOSED
☐ CHARGE TO MY CREDIT CARD
☐ VISA   ☐ MASTERCARD   ☐ AMERICAN EXPRESS

CARD NO.

Expiration date   Signature

Make check payable in U.S. funds to:
AEE ENERGY BOOKS

④ Send your order to:
AEE BOOKS
P.O. Box 1026
Lilburn, GA 30048

INTERNET ORDERING
www.aeecenter.org/books
(use discount code)

TO ORDER BY PHONE
Use your credit card and call:
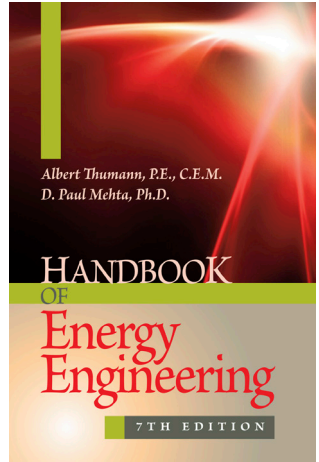**(770) 925-9558**

TO ORDER BY FAX
Complete and Fax to:
(770) 381-9865

INTERNATIONAL ORDERS
Must be prepaid in U.S. dollars and must include an additional charge of $10.00 per book plus 15% for shipping and handling by surface mail.

Handbook of Energy Engineering, Seventh Edition

Albert Thumann, P.E., C.E.M., and D. Paul Mehta, Ph.D..

Here's your step-by-step guide to applying the principles of energy engineering and management to the design of electrical, HVAC, utility, process and building systems for both new design and retrofit. Topics include how to do an energy analysis of any system; electrical system optimization; state of the art lighting and lighting controls; thermal storage; cogeneration; HVAC and building system optimization; compressed air systems; new and emerging technologies, third party financing and much more, including information on software packages from DOE's Best Practices program.

ISBN: 0-88173-650-3

6 x 9, 456 pp., Illus.
Hardcover, Order Code 678

ORDER CODE: 678

CONTENTS

BOOK ORDER FORM ✂

① Complete quantity and amount due for each book you wish to order:

Quantity	Book Title	Order Code	Price	Amount Due
	Handbook of Energy Engineering, Seventh Edition	**678**	**$125.00**	

② Indicate shipping address: CODE: Journal 2013

Applicable Discount

Georgia Residents add 6% Sales Tax

Shipping $10 first book $4 each additional book

TOTAL

NAME (Please print)   BUSINESS PHONE

SIGNATURE (Required to process order)   EMAIL ADDRESS

COMPANY

MEMBER DISCOUNTS—A 15% discount is allowed to AEE members (discounts cannot be combined).

☐ **AEE Member** (Member No._____)

STREET ADDRESS ONLY (No P.O. Box)

CITY, STATE, ZIP

③ Select method of payment:
☐ **CHECK ENCLOSED**
☐ **CHARGE TO MY CREDIT CARD**
☐ *VISA*   ☐ *MASTERCARD*   ☐ *AMERICAN EXPRESS*

CARD NO.

Expiration date   Signature

Make check payable in U.S. funds to: **AEE ENERGY BOOKS**

④ Send your order to:
AEE BOOKS
P.O. Box 1026
Lilburn, GA 30048

INTERNET ORDERING
www.aeecenter.org/books
(use discount code)

TO ORDER BY PHONE
Use your credit card and call:
(770) 925-9558

TO ORDER BY FAX
Complete and Fax to:
(770) 381-9865

INTERNATIONAL ORDERS
Must be prepaid in U.S. dollars and must include an additional charge of $10.00 per book plus 15% for shipping and handling by surface mail.

Mode III: at t = 0.2 sec, the PV system generates power (1500W) more than load active power (1100W) demand. As seen from Figure 12, the grid active power is now negative which means that PV feed extra power generated into the grid. The current direction is reversed as seen from Figure 11 for this time interval.

Mode IV: at t=0.3 sec, the local load on the system is increased keeping PV generated power same. Now the extra load power demand is partly shared by the PV and the grid. Out of total load power of 1550 W PV shares 1500W of power whereas remaining load power and the loss power is shared by the grid.

Mode V: at t=0.4 sec, with the increased load, the PV generated power is decreased to 700W. Accordingly there is change in grid current and active power as seen in Figure 11 and Figure 12. The inverter phase voltage in all these modes of operation is shown in Figure 13.

CONCLUSIONS

This article presents the modeling and simulation of a grid connected PV system. The grid current is injected into the grid through a three-level dual inverter. The active power supplied by the PV system depending on environmental condition is injected into the grid. The local load active power is compensated by the PV system depending upon the PV power generated at the given instant. All the benefits of a multilevel inverter can be used in such a system. Also the control algorithm is very simple and easy to implement. An attempt has been made here to use the dual inverter topology in a grid connected PV system.

References
[1] McDermott T.E. and Dugan R.C.," Distributed generation impact on reliability and power quality indices" in Proc. IEEE Rural Electr. Power Conf., 2002, pp. D3-D3_7.
[2] Kuo Y.C., Liang T.J., Chen J.F., "Novel maximum-power-point-tracking controller for photovoltaic energy conversion system," IEEE Trans. on Industrial Electronics, Vol.48 No.3, June 2001, pp. 594-601.
[3] Bleijs J.A.M., Gow J.A.," Fast maximum power point control of current-fed DC-DC converter for photovoltaic arrays," *Electronics Letters*, Vol. 37, N.1, 4 Jan. 2001, pp.5-6.
[4] Gow J.A., Manning C.D.," Controller management for boost converter systems sourced from solar photovoltaic arrays or other maximum power sources," IEE Proceedings of Electric Power Applications, Vol.147, No. 1, Jan. 2000, pp.15-20.
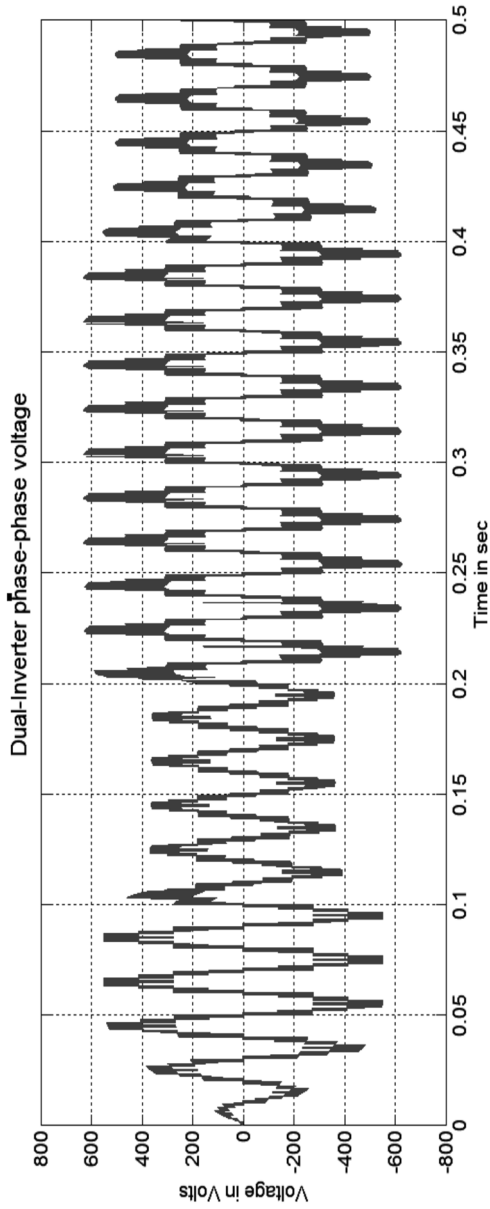
Figure 13. Dual-Inverter output phase-phase voltage

[5] Hua C., Shen C., "Comparative study of Peak Power Tracking Techniques for Solar Storage Systems," IEEE Applied Power Electronics Conference and Exposition Proceedings, Vol 2, pp. 679-683, Feb. 1998.

[6] Bojoi R.I., Limongi L.R., Roiu D., Tenconi A., " Enhanced power quality control strategy for single-phas e inverters in distributed generation systems," IEEE Transaction on Power Electronics, Vol. 26, No. 3, March 2011.

[7] Rodríguez J., Lai J.S., and Zheng Peng F., "Multilevel Inverters: A Survey of Topologies, Controls, and Applications," IEEE Trans. on Ind. Electron., vol. 49, no. 4, pp.724-738, Aug. 2002.

[8] Rodriguez J., Bernet S., Wu Bin, Pontt J.O., and Kouro S., "Multilevel Voltage-Source-Converter Topologies for Industrial Medium-Voltage Drives," IEEE Trans. on Ind. Electron., vol. 54, no. 6, pp. 2930-2945, Dec 2007.

[9] Ostojic Darko, "A multilevel converter structure for grid-connected PV plants," PhD thesis

[10] Koutroulis E., Kalaitzakis K., and Voulgaris N.C., "Development of a microcontroller-based photovoltaic MPPT control system," IEEE TransPower Electron., vol. 16, no. 1, pp. 46-54, Jan. 2001.

[11] Femia N., Petrone G., Spagnuolo G., and Vitelli M., "Optimization of perturb and observe maximum power point tracking method," IEEE Trans. Power Electron., vol. 20, no. 4, pp. 963-973, Jul. 2005.

[12] Buresch M.: *Photovoltaic Energy System Design and Installations*, MGraw-Hill, New York, 1983.

[13] Femia N., Petrone G., Spagnuolo G., and Vitelli M., "Optimizing dutycycle perturbation of P&O MPPT technique," in Proc. 35th Annu. IEEE PESC, Jun. 20–25, 2004, vol. 3, pp. 1939–194.

[14] Selvaraj Jeyraj and Nasrudin A. Rahim, "Multilevel Inverter For Grid-Connected PV System Employing Digital PI Controller," IEEE Transactions On Industrial Electronics,Vol. 56, No. 1, January 2009

[15] Baiju M.R., Mohapatra K.K., Kanchan R.S., and Gopakumar K.: 'A dual two-level inverter scheme with common mode voltage elimination for an induction motor drive', IEEE Trans. Power Electron., 2004, 19, (3), pp. 794–805.

[16] Satheesh G., Bramhananda Reddy T. and Sai babu C.H.: 'Three-level voltage generation for Dual Inverter fed open end winding Induction motor drive' *International Journal of Engineering Science and Technology* (IJEST), Vol. 3 No. 5 May 2011. pp. 3892-3991.

_____

ABOUT THE AUTHORS

Udaykumar R. Yaragatti, member IEEE, is a professor in department of electrical and electronics engineering, National Institute of Technology Karnataka (NITK) Surathkal. He received his PhD in Energy Systems Engineering from Indian Institute of Technology Bombay (IITB) Mumbai in the year 2000. His work experience includes teaching and research in the area of Power Electronics, Solid State Devices, PV systems and Applications, Electrical Machine Design, Electrical Energy Systems, Energy Management and Energy Auditing.

He has published more than 80 technical papers in International and National Journals and Conferences. Email:udaykumarry@yahoo.com

Anant Naik is a research scholar in the department of electrical and electronics engineering, National Institute of Technology Karnataka Surathkal. He received his MTech from NITK in the year 2004. He is a faculty at Goa Engineering College, Farmagudi Goa and has a teaching experience of 10 years. His subjects of interest are Power Electronics, Power Quality and Renewable Energy. Presently he is pursuing his PhD at NITK Surathkal. Email: anantnaik05@gmail.com